31st Annual International Conference of the IEEE EMBS
Minneapolis, Minnesota, USA, September 2-6, 2009

Magnetoacoustic Tomography with Magnetic Induction (MAT-MI) for Electrical Conductivity Imaging

Xu Li, *Student Member,* and Bin He*, *Fellow, IEEE*

***Abstract*—Magnetoacoustic tomography with magnetic induction (MAT-MI) is a recently introduced method for imaging electrical conductivity properties of biological tissue with high spatial resolution close to sonography. In MAT-MI the sample resides in a static magnetic field and a time-varying magnetic stimulation is applied to the sample volume. Through the action of the Lorentz force, the magnetically induced eddy current in the conductive sample causes particle vibrations and generates detectable ultrasound waves. The acoustic signal is then measured around the object to reconstruct images that are related to the object electrical conductivity distribution. The feasibility to reconstruct high spatial resolution conductivity images using MAT-MI method has been demonstrated by both computer simulation and experimental studies. Though MAT-MI technique is still in its developing stage, all the pilot studies suggest that it has potential to become a noninvasive imaging modality for high spatial resolution conductivity imaging of biological tissue and merits further investigations. This paper reviews MAT-MI about its basic theory, reconstruction algorithms and experiment studies. Some technical issues and future research directions are discussed.**

I. Introduction

Noninvasive imaging of electrical impedance of biological tissues has been an active research area for several decades. One of the major advantages of these imaging methods comes from the sensitivity of the electrical impedance properties including conductivity and permittivity to physiological and pathological conditions of living system [1]. In addition, the knowledge of biological tissue impedance is of great interest to researchers doing electromagnetic source imaging [2]. Among all the related techniques, electrical impedance tomography (EIT) [3], [4] was firstly developed using current injection and noninvasive surface voltage measurements. EIT has the benefits of low cost, real-time speed and safety. Its major limitations include low spatial resolution and degraded sensitivity in the center of an object. In addition, as EIT uses current injection through surface electrodes, it has the problem of "shielding effect" [5]. Magnetic induction tomography (MIT) was introduced [6] with both non-contact stimulation and measurement. In MIT, an oscillating magnetic field is applied to the conductive sample and measurements of the secondary magnetic field produced by the induced eddy current are taken by small coils arranged around the object. However, the spatial resolution of current MIT technique is still quite limited. In order to achieve high spatial resolution conductivity imaging, magnetic resonance electrical impedance tomography (MREIT) was developed by combining EIT and magnetic resonance current density imaging (MRCDI) [7], [8]. In MREIT, the magnetic field disturbance caused by the injected current in the conductive sample is measured by a magnetic resonance imaging system. High spatial resolution conductivity images were obtained in both *in vitro* and *in vivo* experiments [8], however MREIT is currently limited by its requirement of high level current injection to obtain acceptable signal-to-noise (SNR) level.

Besides the electromagnetic imaging methods as EIT, MIT and MREIT, an alternative approach for noninvasive imaging of electrical current or conductivity is through the coupling between electromagnetic field and acoustic field as reported in the magnetoacoustic tomography (MAT) [9], [10] and Hall Effect imaging (HEI) [5], [11], [12]. In MAT and HEI, spontaneous or injected current is coupled to acoustic vibrations through the Lorentz force with existence of a static magnetic field.

Recently, magnetoacoustic tomography with magnetic induction (MAT-MI) [13]-[19] was proposed to achieve noninvasive electrical conductivity imaging with high spatial resolution. MAT-MI utilizes magnetic induction to induce eddy current in the conductive sample and generate acoustic vibrations through the same Lorentz force coupling mechanism as in MAT/HEI. The feasibility of MAT-MI method to reconstruct high resolution conductivity related images has been demonstrated by both computer simulation and experimental studies.

II. Problem Description

A. Forward Problem

The forward problem describes two major physical processes in the signal generation mechanism of MAT-MI i.e. magnetic induction in the conductive sample and the acoustic wave propagation with the Lorentz force induced acoustic sources.

We consider a sample with isotropic conductivity $\sigma(\mathbf{r})$. The sample is placed in a static magnetic field with flux

Manuscript received Apr 17, 2008. This work was supported in part by NIH R21EB006070, NSF BES-0602957, NIH RO1EB007920, NIH RO1 HL080093, and a grant from the Institute for Engineering in Medicine of the University of Minnesota.

B He is with the University of Minnesota, Minneapolis, MN 55455 USA (* Corresponding author phone: 612-626-1115; e-mail: binhe@umn.edu).

X Li is with the University of Minnesota, Minneapolis, MN 55455 USA (e-mail: lixxx317@umn.edu).

density $\mathbf{B}_0(\mathbf{r})$. A time varying magnetic field $\mathbf{B}_1(\mathbf{r},t)$ is applied to the sample and induces electrical field $\mathbf{E}(\mathbf{r},t)$ and eddy current density $\mathbf{J}(\mathbf{r},t)$ in its conductive volume.

As in MAT-MI we are considering around μs level current pulses for driving the stimulating coil, the corresponding mega Hz skin depth in general biological tissue is at the level of meters, so the magnetic induction problem in MAT-MI can be considered quasistatic and magnetic diffusion can be ignored. This condition allows us to separate the spatial and temporal function of the time-varying magnetic field, i.e. $\mathbf{B}_1(\mathbf{r},t) = \mathbf{B}_1(\mathbf{r}) f(t)$. It also indicates that the stimulating magnetic field in the sample can be well approximated by the field generated by the same coil configuration in free space [20]. In addition, the displacement current can be ignored as it is much smaller than the conductive current in biological tissue at mega Hz frequency [14]. Using the notations of magnetic vector potential $\mathbf{A}(\mathbf{r},t)$ where $\mathbf{B}_1 = \nabla \times \mathbf{A}$ and electrical scalar potential $\varphi(\mathbf{r})$, the governing equation for magnetic induction in MAT-MI can be written as in (1) [16]

$$\nabla \cdot (\sigma(-\frac{\partial \mathbf{A}}{\partial t} - \nabla\varphi)) = 0 \tag{1}$$

This equation subject to a Neumann boundary condition on the current density $\mathbf{J}$ as in (2) can be solved throughout the conductive volume by using finite element methods (FEM) [20]

$$\mathbf{J} \cdot \mathbf{n} = 0 \tag{2}$$

where $\mathbf{n}$ is the norm of the outer boundary surface. In a simple conductive geometry as concentric spheres, this magnetic induction problem has an analytical solution as shown in [16]. For simplicity, in the following part, we assume $\mathbf{J}(\mathbf{r},t) = \mathbf{J}(\mathbf{r})\delta(t)$, which according to Faraday's Law indicates $f(t) = u(t)$, where $u(t)$ is a step function.

With the magnetically induced eddy current $\mathbf{J}$ and the static magnetic field $\mathbf{B}_0$, the Lorentz force acting on the eddy current can be described as $\mathbf{J} \times \mathbf{B}_0$. In MAT-MI the divergence of the Lorentz force acts as acoustic source of propagating ultrasound wave which is sensed by ultrasonic transducers placed around the sample. The wave equation governing the pressure distribution is given in (3) [10]

$$\nabla^2 p - \frac{1}{c_s^2}\frac{\partial^2 p}{\partial t^2} = \nabla \cdot (\mathbf{J}(\mathbf{r}) \times \mathbf{B}_0) \tag{3}$$

where p is the pressure and c_s is the acoustic speed in the media. Here we assume the sample is acoustically homogeneous, i.e. the acoustic speed is a constant. Using Green's function, the solution to (3) can be written as in (4)

$$p(\mathbf{r}',t) = -\frac{1}{4\pi}\int_V d\mathbf{r} \nabla_{\mathbf{r}} \cdot [\mathbf{J}(\mathbf{r}) \times \mathbf{B}_0] \frac{\delta(t - R/c_s)}{R} \tag{4}$$

where $R = |\mathbf{r} - \mathbf{r}'|$, and V is the volume containing the acoustic sources. It is shown in (4) that the pressure field p at location $\mathbf{r}'$ and at time t, is proportional to the integration of the source term $\nabla \cdot (\mathbf{J}(\mathbf{r}) \times \mathbf{B}_0)$ over a spherical surface centered at $\mathbf{r}'$ with the radius to be tc_s.

B. Inverse Problem

The inverse problem of MAT-MI describes how to reconstruct the conductivity distribution $\sigma(\mathbf{r})$ from the pressure field measurement p that we can measure around the sample.

III. Reconstruction Algorithms

A. Acoustics Source Reconstruction Algorithm

In this algorithm, the acoustic source term $\nabla \cdot (\mathbf{J}(\mathbf{r}) \times \mathbf{B}_0)$ of the wave equation is firstly reconstructed using the time reversal technique as in (5) [14]

$$\nabla \cdot (\mathbf{J}(\mathbf{r}) \times \mathbf{B}_0) \approx \frac{-1}{2\pi c_s^2}\iint_{\Sigma} dS_d \frac{\mathbf{n}_d \cdot (\mathbf{r}_d - \mathbf{r})}{|\mathbf{r} - \mathbf{r}_d|^2} \cdot \tilde{p}''(\mathbf{r}_d, |\mathbf{r} - \mathbf{r}_d|/c_s)/c_s \tag{5}$$

where $\mathbf{r}_d$ is the location vector on the detection surface Σ on which acoustic transducers are placed, $\mathbf{n}_d$ is the normal vector of Σ at $\mathbf{r}_d$, and $\mathbf{r}$ is the location vector of the source. The double prime refers to the second derivative over time. With the reconstructed source term, the conductivity distribution $\sigma(\mathbf{r})$ can be further estimated as in (6) [14]

$$\sigma(\mathbf{r}) \approx -\frac{\nabla \cdot (\mathbf{J}(\mathbf{r}) \times \mathbf{B}_0)}{\mathbf{B}_1(\mathbf{r}) \cdot \mathbf{B}_0} \tag{6}$$

where the approximation comes from a piecewise homogeneous assumption on the conductivity distribution and the equation does not hold on those conductivity boundaries. Computer simulations using concentric spherical conductivity models have shown that this algorithm can reconstruct the conductivity values in each smooth area with less than 5% relative error [16], however, median filter has to be used to remove those boundary errors caused by the approximation. In all the experiment studies described in section IV, this acoustic source reconstruction algorithm was used.

B. Vectorial field Reconstruction Algorithm

This algorithm is based on the recently proposed vectorial field reconstruction method [19]. Basically, we have demonstrated in theory and numerical simulation that by vectorizing the scalar pressure measurements on spherical or cylindrical measurement geometry, a curl-free vectorial field whose divergence serves as acoustic source can be reconstructed directly from these pressure measurements. Applying this to MAT-MI and assuming the static magnetic field is in Z direction, if the induced eddy current density changes slowly in Z direction, the Lorentz force field will satisfy the curl-free condition and the reconstruction algorithm for the Lorentz force field with a cylindrical

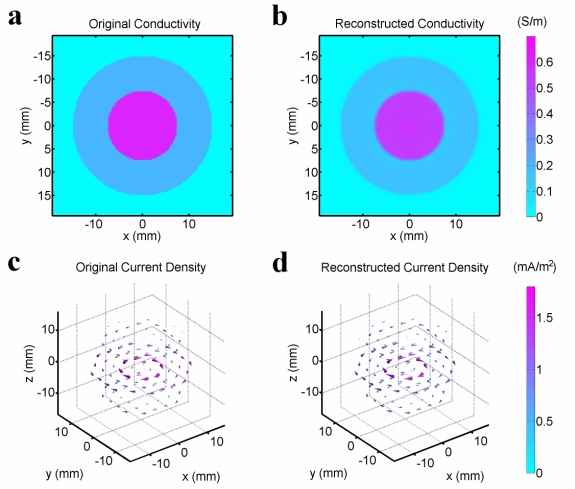

Fig. 1. MAT-MI Simulation results using the vector field reconstruction algorithm and a concentric spherical conductivity model. (a) and (b) are original and reconstructed conductivity distributions at Z=0 slice. (c) and (d) are original and reconstructed current density distribution [19].

measurement geometry is given in (7) [19]

$$|\mathbf{F}(\rho,\varphi,z)|\exp(i\theta_{\mathbf{F}}) = -\frac{1}{2\pi c^3}\iint_{S_0} dS_0 \cdot \sqrt{1-\frac{(z_0-z)^2}{|\mathbf{r}-\mathbf{r}_0|^2}}\,\frac{1}{t}\,\frac{\partial p(\mathbf{r}_0,t)}{\partial t}\Big|_{t=|\mathbf{r}-\mathbf{r}_0|/c}\exp(i\theta_0) \tag{7}$$

where θ_0 and $\theta_{\vec{F}}$ are the azimuth of the vectors $\mathbf{r}_0$ and $\mathbf{F}$, respectively. $\mathbf{F} = \mathbf{J}(\mathbf{r})\times\mathbf{B}_0$ is the Lorentz force field in the conductive sample. $\mathbf{r}_0$ is the location vector of the cylindrical measurement surface S_0. With the reconstructed Lorentz force field and known static magnetic field, the eddy current density distribution can be easily obtained. In some simple geometry as in the concentric spherical model, assuming the electric field $\mathbf{E}$ is similar to that induced in a uniform conductive media, we can still get a good conductivity reconstruction as compared to the acoustic source reconstruction algorithm [19]. A simulation result using this algorithm is shown in Fig. 1. The feasibility of this algorithm has not been verified by experiment data yet.

IV. Experiment Study

A. Experiment System

We have developed both 2D and 3D MAT-MI systems for our experiment studies. In these systems, permanent magnets are used to give the static field with strength of 0.1T near the sample. The time varying magnetic stimulation is sent through a single coil or a pair of Helmholtz coil driven by home-made magnetic stimulators. The transducer is flat and centered at 500 KHz. The transducer is mounted to a frame and can do circular scanning in the horizontal plane (the XY plane) [15]. In the 3D system, it can also move in the vertical direction (the Z direction) with acoustic focusing lens placed in front of it [17]. Ultrasound signals is pre-amplified and digitized at 5 MHz.

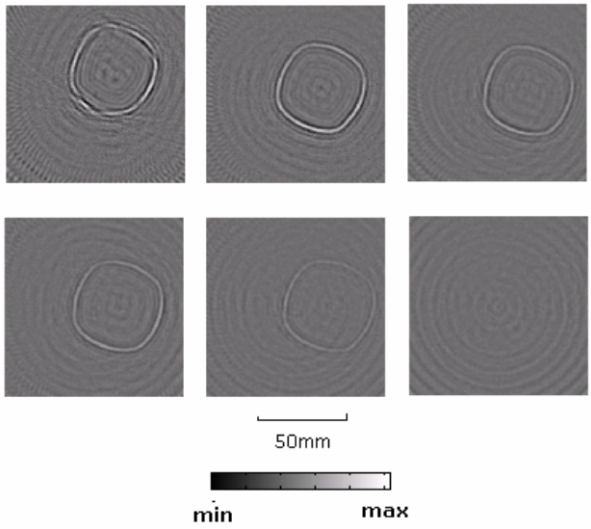

Fig. 2. MAT-MI images of saline phantoms with salinity to be 10%, 8%, 5%, 3%, 1% and 0% from left to right and from top to bottom [15].

B. Imaging Results

We have conducted MAT-MI imaging experiments on metal object [14], saline, gel phantoms [15] and biological tissue phantoms [17].

MAT-MI images of saline samples with different salinities are shown in Fig. 2. The saline samples are put in a plastic cup and emerged in water. The transducer scans the sample with a 2.5° step. The conductivity boundaries are well reconstructed in consistent with the sample geometry. It is also shown in this result that the boundary intensities in the reconstructed MAT-MI images are in positive correlation with the phantom's salinity thus the conductivity contrast between the saline sample and background [15].

Imaging results of two tissue phantoms are shown in Fig. 3. Figures 3 (a) and (b) illustrate the photo and reconstructed MAT-MI image of a salt pork tissue phantom. Figures 2 (c) and (d) are from a tissue phantom made from fresh pork muscle and fat. It is shown in Fig. 2 that the MAT-MI images are consistent with the tissue phantom geometry. Because the conductivity of muscle tissue is quite different from that of fat tissue, the boundaries between these two types of tissue are clearly seen in the reconstructed images. The spatial resolution is 3mm for each image.

V. Discussion

We have conducted theoretical and experimental studies to demonstrate the feasibility of the newly proposed MAT-MI method for noninvasive high resolution conductivity imaging. In principle, MAT-MI has advantages in its high spatial resolution as compared to EIT and MIT and void of shielding effect as compared with other magnetoacoustic imaging approach such as MAT/HEI. This method also has a well-posed inverse problem as the acoustic source can be

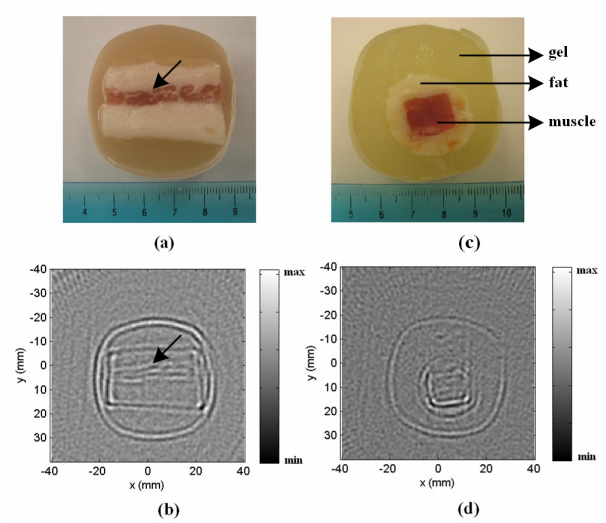

Fig. 3. MAT-MI images of biological tissue phantoms. (a) photo of a salt pork tissue sample, (c) photo of a pork tissue sample composed of a block of pork muscle embedded in a cylindrical fat layer. The surrounding material is animal gelatin. (b) and (d) are reconstructed MAT-MI images of the sample shown in (a) and (c) respectively [17].

reconstructed on each point in the conductive sample [14]. Potential applications of MAT-MI include breast cancer detection and cancer screening in other soft tissues.

In all the reconstruction algorithms developed for MAT-MI, in order to give a complete and accurate reconstruction, wide band signals must be collected from full acoustic view angles, i.e. 4 π solid angle for 3D reconstruction. However, in practice, these two conditions can hardly be met, as most ultrasound transducers have limited bandwidth, and the acoustic window is quite limited for most biomedical applications [11]. These effects need to be taken into account in the data preprocessing method and reconstruction algorithms developed later. In addition, the boundary errors existed in the acoustic source reconstruction algorithm remains to be addressed as shown in the simulation study in [16]. Experiment results also indicate the importance of considering the acoustic source generated at conductivity boundaries in the MAT-MI signal modeling and corresponding reconstruction algorithm development. We are developing new algorithms to solve this issue. The acoustic homogeneous assumption used in all the reconstruction algorithms would limit the MAT-MI technique to soft tissue imaging. Furthermore, conductivity anisotropy will cause different acoustic source pattern compared to the corresponding isotropic case [18]. This anisotropic effect will not affect the acoustic source reconstruction, however it would introduce errors in the reconstructed conductivity. This issue needs to be addressed in the future research.

REFERENCES

[1] L. A. Geddes and L. E. Baker, "The specific resistance of biological materials: A compendium of data for the biomedical engineer and physiologist," *Med. Biol. Eng.*, vol. 5, pp. 271–293, 1967

[2] B. He, *Modeling and Imaging of Bioelectrical Activity – Principles and Applications*, Kluwer Academic Publishers, 2004.

[3] P. Metheral, D. C., Barber, R. H. Smallwood, B. H. Brown, "Three-dimensional electrical impedance tomography," *Nature*, vol. 380, pp. 509-512, 1996.

[4] M. Cheney, D. Isaacson and J. C. Newell, "Electrical Impedance Tomography," *SIAM Review.,* vol. 41, pp. 85-101, 1999.

[5] H. Wen, J. Shah, and S. Balaban, "Hall effect imaging," *IEEE Trans. Biomed. Eng.,* vol. 45, pp. 119-124, Jan. 1998.

[6] H. Griffiths, "Magnetic Induction tomography", *Meas. Sci. Technol.*, vol. 12, pp. 1126-1131, 2001.

[7] M. Joy, G. Scott and M. Henkelman, "In vivo detection of applied electric currents by magnetic resonance imaging", *Magnetic Resonance Imaging*, vol. 7, pp. 89-94, 1989.

[8] E. J. Woo and J. K. Seo, "Magnetic resonance electrical impedance tomography (MREIT) for high-resolution conductivity imaging," *Physiol. Meas.,* vol. 29, pp. R1-R26, 2008.

[9] B. C. Towe and M.R. Islam, "A magneto-acoustic method for the noninvasive measurement of bioelectric currents," *IEEE Trans. Biomed. Eng.,* vol. 35, pp. 892-894, Oct. 1988.

[10] B. J. Roth, P. J. Basser and J. P. Jr Wikswo, "A theoretical model for magneto-acoustic imaging of bioelectric currents", *IEEE Trans. Biomed. Eng*., vol. 41, pp. 723–728, Aug. 1994.

[11] H. Wen, "Feasibility of biomedical application of Hall effect imaging," *Ultrason. Imaging*, vol. 22, pp. 123-136, 2000.

[12] A. Montalibet, J. Jossinet, A. Matias and D. Cathignol, "Electric current generated by ultrasonically induced Lorentz force in biological media,", *Med. & Bio. Eng. Comput*, vol. 39, pp. 15-20, Jan. 2001.

[13] B. He, "High-resolution functional source and impedance imaging," *Proc. Annu. Int. Conf. IEEE-EMBS*, pp. 4178–4182, 2005.

[14] Y. Xu and B. He, "Magnetoacoustic tomography with magnetic induction," *Phys. Med. Biol.*, vol. 50, pp. 5175-5187, 2005.

[15] X. Li, Y. Xu, and B. He, "Magnetoacoustic tomography with magnetic induction for imaging electrical impedance of biological tissue," *J. Appl .Phys.*, vol. 99, 066112, 2006.

[16] X. Li, Y. Xu, and B. He, "Imaging electrical impedance from acoustic measurements by means of magnetoacoustic tomography with magnetic induction (MAT-MI)," *IEEE Trans. Biomed. Eng.,* vol. 54, pp. 323-330, Feb. 2007.

[17] R. Xia, X. Li, and B. He, "Magnetoacoustic tomographic imaging of electrical impedance with magnetic induction," *Appl. Phys. Lett.*, vol. 91, 083903, 2007.

[18] K. Brinker and B. J. Roth, "The Effect of Electrical Anisotropy During Magnetoacoustic Tomography With Magnetic Induction", *IEEE Trans. Biomed. Eng.*, vol.55, no. 5, pp. 1637-1639, May 2008.

[19] R. Xia, X. Li, and B. He, "Reconstruction of Vectorial Acoustic Sources in Time-Domain Tomography", *IEEE Trans. Med. Imaging*, vol. 28, pp. 669–675, May 2009.

[20] W. Wang and S. R. Eisenberg, "A Three-Dimensional Finite Element Method for Computing Magnetically Induced Currents in Tissues," *IEEE Trans. Magn.*, vol. 30, pp. 5105-5023, Nov. 1994.